

## **Dynamics of Adsorption from Micellar Surfactant Solutions at Expanding Fluid Interfaces in Relation to the Emulsification Process**

Krassimir D. Danov\*,<sup>†</sup> Peter A. Kralchevsky,<sup>†</sup> Nikolai D. Denkov,<sup>†</sup>  
Kavssery P. Ananthapadmanabhan,<sup>§</sup> and Alex Lips<sup>§</sup>

<sup>†</sup>*Laboratory of Chemical Physics and Engineering, Faculty of Chemistry, University of Sofia, 1164 Sofia, Bulgaria*

<sup>§</sup>*Unilever Research & Development, Trumbull, Connecticut 06611, USA*

**Abstract.** A detailed theoretical model of micellar kinetics is developed and applied to the case of surfactant adsorption at fluid interfaces. The adsorption gives rise to diffusion of surfactant monomers and micelles, and to release of monomers by the micelles. The numerical solution of the problem reveals the existence of four distinct kinetic regimes. At the greatest expansion rates (lowest surface age), the surfactant adsorption is affected by the fast micellar process (regime AB). At smaller expansion rates, the fast process equilibrates and the adsorption occurs under diffusion control (regime BC). With the further decrease of the expansion rate, the surfactant adsorption is affected by the slow micellar process (regime CD). Finally, at the lowest expansion rates, both the fast and slow micellar processes are equilibrated, and the adsorption again occurs under diffusion control (regime DE). For each separate kinetic regime, convenient analytical expressions for the dynamic interfacial tension and adsorption are derived. At low micelle concentrations, “rudimentary” kinetic diagrams are observed, which are characterized by merging or disappearance of the regimes BC and CD. Usually, only one of the kinetic regimes is experimentally detected. The developed theoretical model enables one to identify which of the four regimes is observed in a given experiment, and to interpret properly the obtained data. We applied the model to process available and new data obtained by means of various experimental methods for dynamic interfacial tension. Very good agreement between theory and experiment is achieved. A quantitative criterion is developed, which shows whether a given emulsifier is “fast” or “slow”.

**Keywords:** micellar surfactant solutions; fast and slow micellization processes; adsorption kinetics of surfactants; dynamic surface tension; diffusion in micellar surfactant solutions.

\***Corresponding author:** Krassimir D. Danov, E-mail: [kd@lcpe.uni-sofia.bg](mailto:kd@lcpe.uni-sofia.bg)

## 1. Introduction

The process of emulsification is accompanied by drop breakage and adsorption of surfactant at the newly formed oil-water interface. If the characteristic time of surfactant adsorption is shorter than the average drop-drop collision time, then the drop surfaces will be covered by protective adsorption monolayers and the collisions will not lead to drop coalescence. In the opposite case, the drops will coalesce, and a coarse and/or unstable emulsion will be produced. Hence, the kinetics of surfactant adsorption plays a crucial role in emulsification.

In emulsification, most frequently surfactant concentrations above the critical micellization concentration (CMC) are used. In such case, both surfactant monomers and micelles take part in the diffusion process (Fig. 1). The micelles release monomers and could decompose in order to compensate the monomers adsorbed at the interface. The role of the micelles as sources and carriers of monomers leads to a marked acceleration of surfactant adsorption.

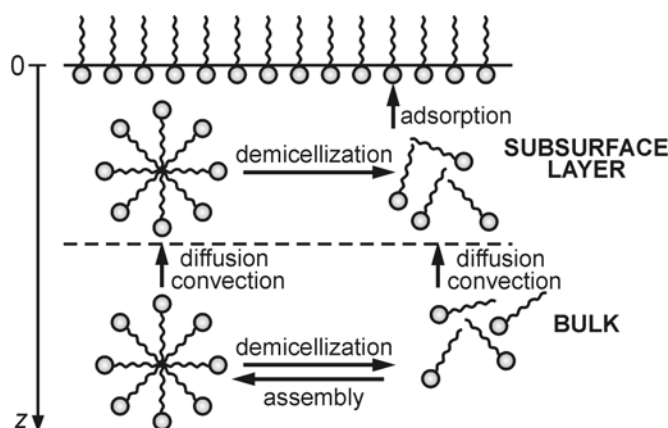


**Fig. 1.** The process of surfactant adsorption from micellar solutions. In the neighborhood of an expanded adsorption monolayer, the micelles release monomers to restore the equilibrium surfactant concentration at the surface and in the bulk. The concentration gradients give rise to bulk diffusion of both monomers and micelles.

The first models of micellar kinetics in spatially uniform solutions have been developed by Kresheck et al. (1) and Aniansson and Wall (2). The existence of “fast” and “slow” processes of the micellar dynamics has been established. The first theoretical model of surfactant adsorption from micellar solutions, proposed by Lucassen (3), uses the simplifying assumptions that the micelles are monodisperse, and that the micellization happens as a single step, which is described as a reversible reaction of order  $n$  (the micelle aggregation number). Later, more realistic models, which account for the multi-step character of the micellar process, were developed (4-6). The assumption for a complete local dynamic equilibrium between monomers and micelles makes possible to use the equilibrium mass-action law for the micellization

reaction (3,7,8). In such a case, the surfactant transfer corresponds to a conventional diffusion-limited adsorption characterized by an effective diffusion coefficient,  $D_{\text{eff}}$ , which depends on the micelle diffusivity, concentration and aggregation number (7,8).  $D_{\text{eff}}$  is independent of the rate constants of the fast and slow demicellization processes:  $k_m$  and  $k_s$ . Joos et al. (7,8) confirmed experimentally that in some cases the adsorption from micellar solutions could be actually described as a diffusion-limited process characterized by an apparent diffusivity,  $D_{\text{eff}}$ . In other experiments, Joos et al. (9,10) established that sometimes the dynamics of adsorption from micellar solutions exhibits a completely different kinetic pattern: the interfacial relaxation is exponential, rather than inverse-square-root, as it should be for diffusion-limited kinetics. The theoretical developments (9-11) revealed that the exponential relaxation is influenced by the kinetics of micellization, and from the data analysis one could determine the rate constant of the fast process,  $k_m$ . The observation of different kinetic regimes for different surfactants and/or experimental methods makes the physical picture rather complicated.

Recently, we proposed a new realistic model of the micellar kinetics (12), and applied it to investigate the dynamics of adsorption at quiescent (13) and expanding (14,15) interfaces. The theoretical analysis reveals the existence of four different consecutive relaxation regimes (stages) for a given micellar solution: two exponential regimes and two inverse-square-root regimes, following one after another in alternating order. Here, the results of these studies are summarized, the theoretical predictions are presented, and the agreement between theory and experiment is illustrated.

## 2. The four kinetic regimes of adsorption from micellar solutions

In Refs. (12,13), we proposed a theoretical model, which generalizes previous models of micellization kinetics in several aspects. We avoided the use of the quasi-equilibrium approximation (local chemical equilibrium between micelles and monomers). The theoretical problem was reduced to a system of four nonlinear differential equations. In Ref. (13), the theoretical model was applied to the case of surfactant adsorption at a quiescent interface, i.e. to the relaxation of surface tension and adsorption after a small initial perturbation. Computer modeling of the adsorption process, based on the derived full system of equations, was carried out.

Let us define the perturbations in the basic parameters of the micellar solution:

$$\xi_1 \equiv \frac{h_a}{\Gamma_{p,0}} c_{1,p}; \quad \xi_c \equiv \frac{h_a}{\beta \Gamma_{p,0}} C_{m,p}; \quad \xi_m \equiv \frac{h_a c_{1,\text{eq}}}{\sigma_{\text{eq}}^2 \Gamma_{p,0}} m_p \quad [1]$$

Here,  $c_{1,p}$ ,  $C_{m,p}$  and  $m_p$  are, respectively, the perturbations in the monomer concentration,  $c_1$ , micelle concentration,  $C_m$ , and in the micelle mean aggregation number,  $m$ ; the respective *dimensionless* perturbations are  $\xi_1$ ,  $\xi_c$  and  $\xi_m$ ;  $\Gamma_{p,0}$  is the

perturbation in the surfactant adsorption at the initial moment ( $t = 0$ );  $\sigma_{\text{eq}}$  is the halfwidth of the equilibrium micelle size distribution modeled by a Gaussian bell-like curve;  $\beta$  and  $h_a$  are, respectively, the dimensionless bulk micelle concentration and the characteristic adsorption length, defined as follows:

$$\beta \equiv (C_{\text{tot}} - \text{CMC})/\text{CMC}; \quad h_a = (d\Gamma/dc_1)_{\text{eq}} \quad [2]$$

where  $C_{\text{tot}}$  is the total surfactant concentration;  $\Gamma$  is the surfactant adsorption. The dimensionless fluxes of the fast and slow demicellization processes, denoted by  $\varphi_m$  and  $\varphi_s$ , respectively, can be expressed as follows (13):

$$\varphi_m = \xi_1 - \xi_m \quad [3]$$

$$\varphi_s = (m_{\text{eq}} - w\sigma_{\text{eq}})\xi_1 - m_{\text{eq}}\xi_c + \sigma_{\text{eq}}w\xi_m \quad [4]$$

(Some small terms are neglected in Eqs. [3-4].) Here  $m_{\text{eq}}$  is the equilibrium micelle aggregation number, and  $w = (m_{\text{eq}} - n_r)/\sigma_{\text{eq}}$ , where  $n_r$  is an aggregation number at the boundary between the regions of the rare aggregates and the abundant micelles (13).

Fig. 2 shows results obtained by solving numerically the general system of equations in Ref. (13) for a relatively high micelle concentration,  $\beta = 100$ . The calculated curves  $\xi_{1,0}(\tau)$ ,  $\xi_{c,0}(\tau)$ , and  $\xi_{m,0}(\tau)$  represent the subsurface values (at  $z = 0$ , Fig. 1) of the perturbations  $\xi_1$ ,  $\xi_c$  and  $\xi_m$ , plotted versus the dimensionless time,  $\tau = (D_1/h_a^2)t$ , where  $D_1$  is the diffusion coefficient of the surfactant monomers. Note that  $\xi_{1,0}$  expresses not only the perturbation in the subsurface monomer concentration, but also the perturbations in the surface tension and adsorption (13):

$$\frac{\gamma(t) - \gamma_{\text{eq}}}{\gamma(0) - \gamma_{\text{eq}}} = \frac{\Gamma(t) - \Gamma_{\text{eq}}}{\Gamma(0) - \Gamma_{\text{eq}}} = \xi_{1,0}(\tau) \quad [5]$$

$\gamma(t)$  and  $\Gamma(t)$  are the dynamic surface tension and adsorption;  $\gamma(0)$  and  $\Gamma(0)$  are their initial values, and  $\gamma_{\text{eq}}$  and  $\Gamma_{\text{eq}}$  are their final equilibrium values. A typical value,  $k_m/k_s = 10^7$ , of the ratio of the rate constants of the fast and slow demicellization processes is used to calculate the curves in Fig. 2.

The most important feature of the relaxation curves in Fig. 2, which represents a kinetic diagram, is that  $\xi_{m,0}$  merges with  $\xi_{1,0}$  at a given point, denoted by B, while  $\xi_{c,0}$  merges with  $\xi_{1,0}$  (and  $\xi_{m,0}$ ) at another point, denoted by D. The time moments, corresponding to the points B and D, are denoted by  $\tau_B$  and  $\tau_D$ , respectively. As seen in Fig. 2, for  $\tau > \tau_B$ , we have  $\xi_{1,0} = \xi_{m,0}$ . In view of Eq. [3], this means that for  $\tau > \tau_B$  the flux of the fast micelle relaxation process,  $\varphi_m$  is equal to zero. In other words, for  $\tau > \tau_B$  the monomers and micelles are equilibrated with respect to the *fast* micellar process. It

turns out that for a regular relaxation process  $\tau_B = \sigma_{\text{eq}} h_a (2k_m/D_1)^{1/2}$ ; see Ref. (13). In addition, for  $\tau > \tau_D$  we have  $\xi_{c,0} = \xi_{1,0} = \xi_{m,0}$ , and then Eq. [4] indicates that  $\varphi_s = 0$ , i.e. the monomers and micelles are equilibrated with respect to the *slow* micellar process.

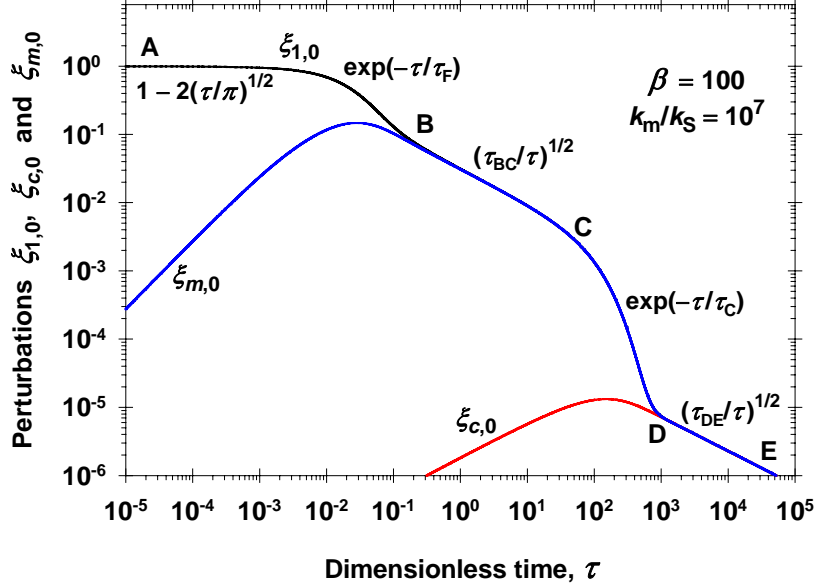


**Fig. 2.** Time dependence of the perturbations in the subsurface monomer concentration,  $\xi_{1,0}$ , micelle concentration,  $\xi_{c,0}$ , and mean aggregation number,  $\xi_{m,0}$ , for  $\beta = 100$ . The curves are obtained by numerical solution of the general system of equations in (13).

The computer modeling (13) shows that  $\xi_{1,0}(\tau)$  exhibits two exponential (kinetic) regimes, AB and CD, and two inverse-square-root (diffusion) regimes, BC and DE, see Fig. 2. In particular, the point C corresponds to the moment  $\tau_C = (D_1/h_a^2)t_c \approx (\beta D_1 \sigma_{\text{eq}}^2)/(k_s h_a^2 m_{\text{eq}}^3)$ , where  $t_c$  is the characteristic time of the slow micellar process; see Ref. (12).  $\tau_C$  serves also as a characteristic relaxation time of adsorption in the kinetic regime CD. The expressions for the other characteristic times,  $\tau_F$ ,  $\tau_{BC}$  and  $\tau_{DE}$  (Fig. 2) are (13):

$$\tau_F = (m_{\text{eq}} D_1)/(\beta k_m h_a^2) \quad (\text{regime AB}) \quad [6]$$

$$\frac{1}{\tau_{BC}} = \frac{D_{BC}}{D_1} = (1 + u\beta)(1 + u\beta B_m) \quad (\text{regime BC}) \quad [7]$$

$$\frac{1}{\tau_{DE}} = \frac{D_{DE}}{D_1} = [1 + (u + m_{\text{eq}})\beta][1 + (u + m_{\text{eq}})\beta B_m] \quad (\text{regime DE}) \quad [8]$$

Here,  $D_{BC}$  and  $D_{DE}$  are the effective diffusivities of the micellar solutions in the regimes BC and DE, respectively;  $u = \sigma_{\text{eq}}^2/m_{\text{eq}}$  and  $B_m = D_m/D_1$ ;  $D_m$  is the mean diffusivity of the micelles. Typical parameter values are  $u \approx 1$  and  $B_m \approx 0.2$ .

It should be noted that in addition to the regular kinetic diagrams (Fig. 2), for low micelle concentrations ( $\beta$  close to 1) one could observe “rudimentary” kinetic diagrams, characterized by merging or disappearance of the stages BC and CD; see Refs. (13) and (14).

The diffusion regimes BC and DE can be observed not only for adsorption at a quiescent interface, but also in the cases of stationary (14) and non-stationary (15) expansion of an interface. The expressions for the effective diffusivities,  $D_{BC}$  and  $D_{DE}$ , given by Eqs. [7] and [8], are valid in all these cases. In particular, the experimental data by Lucassen (3) correspond to the kinetic regime DE, while the experimental data by Joos et al (8) correspond to the kinetic regime BC.

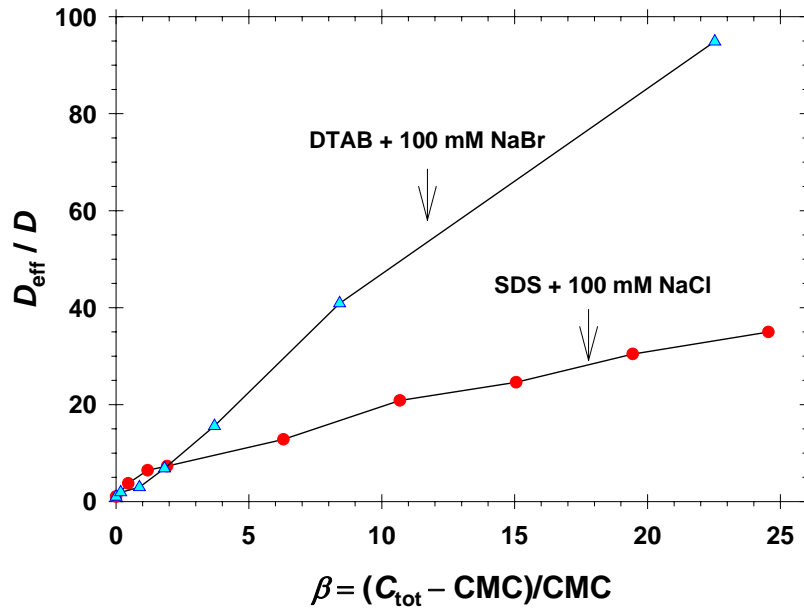


**Fig. 3.** Plot of the dimensionless effective diffusivity of the micellar solution,  $D_{eff}/D$ , vs.  $\beta$ : data obtained in Ref. (15) by means of the maximum bubble pressure method. The lines are guides to the eye.

As an illustration, in Fig. 3 we show experimental data for the ionic surfactants sodium dodecyl sulfate (SDS) and dodecyl trimethyl ammonium bromide (DTAB) + 100 mM added inorganic electrolyte. The data are obtained by means of the maximum bubble pressure method in Ref. (15). To check whether the kinetic regime is DE, we substitute typical parameter values in Eq. [8]:  $m_{eq} = 70$ ,  $\beta = 20$ , and  $B_m = 0.2$ , and as a result we obtain  $D_{DE}/D_1 = 3.9 \times 10^5$ , which is much greater than the experimental values of  $D_{eff}/D$  in Fig. 3. Consequently, the kinetic regime cannot be DE. On the other hand, a similar estimate of  $D_{BC}/D_1$  from Eq. [7] gives reasonable values. To demonstrate that, from the experimental values of  $D_{eff}/D$  in Fig. 3, we calculated  $u$  by means of Eq. [7], substituting  $B_m = 0.2$ . For most of the concentrations we obtain values  $0.4 < u < 2$ ,

which seem reasonable. Values  $u > 2$  are obtained at  $\beta < 2$ , which indicate that at the lowest micellar concentrations we are dealing with a rudimentary kinetic regime (13,14), rather than with the diffusion regime BC.

### 3. The case of stationary interfacial expansion

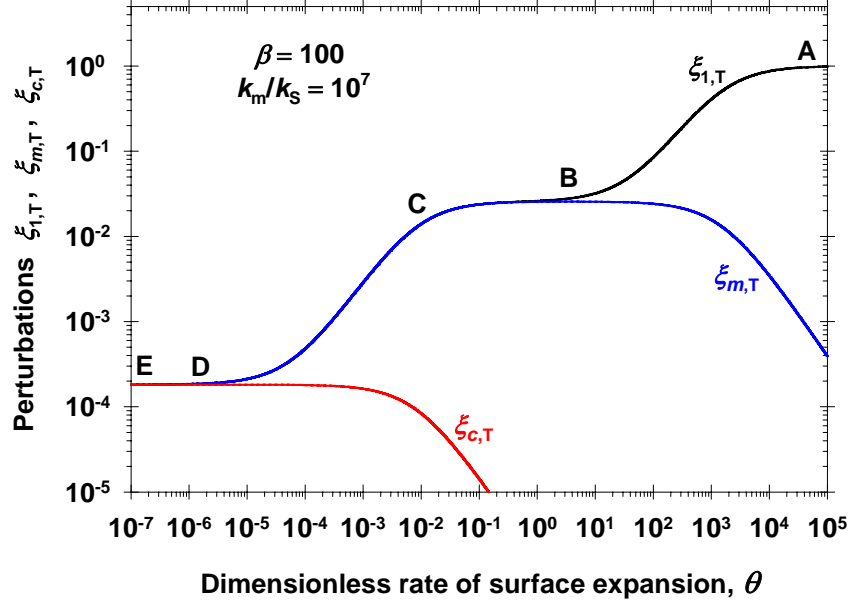


**Fig. 4.** Total perturbations in monomer concentration,  $\xi_{1,T}$ , micelle concentration,  $\xi_{c,T}$ , and mean aggregation number,  $\xi_{m,T}$ , plotted vs. the dimensionless rate of surface expansion,  $\theta$ , for  $\beta = 100$ . The curves are obtained by numerical solution of the linear system in Ref. (14).

This special case of interfacial dynamics is realized with the strip method (8,9) and the overflowing cylinder method (16). Because the adsorption process is stationary, the time,  $t$ , is not a parameter of the state of the system. For this reason, in the kinetic diagrams (like Fig. 4) we plot the perturbations versus the dimensionless rate of surface expansion,  $\theta = (h_a^2/D_1)(dA/dt)/A$ , where  $A$  is the interfacial area, and  $dA/dt = \text{const.}$  is the interfacial expansion rate. In Fig. 4, the total perturbations,  $\xi_{1,T}$ ,  $\xi_{c,T}$  and  $\xi_{m,T}$  are plotted, which represent the local perturbations,  $\xi_1(z)$ ,  $\xi_c(z)$  and  $\xi_m(z)$ , integrated with respect to the normal coordinate  $z$  along the whole semi-axis  $z > 0$  (Fig. 1). As seen in Fig. 4, one observes the same kinetic regimes, as in Fig. 2, although the diagrams in the two figures look like mirror images: the "young" surface age (the regime AB) corresponds to the left side of Fig. 2, but to the right side of Fig. 4. Analytical expressions for the adsorption and surface tension relaxation could be found in Ref. (14). As mentioned above, the expressions for the effective diffusivities,  $D_{BC}$  and  $D_{DE}$ , given by Eqs. [7] and [8], are valid also in the case of stationary interfacial expansion.

In particular, in Ref. (14) we found that the kinetic regime of adsorption from the solutions of the nonionic surfactant polyoxyethylene-20 hexadecyl ether (Brij 58), measured by means of the strip method (8), corresponds to the regime BC.

We recall that in the regime BC the rate constants of the fast and slow micellar processes,  $k_m$  and  $k_s$ , do not affect the surfactant adsorption kinetics, and cannot be determined from the fit of the data. In principle, it is possible to observe the kinetic regime AB (and to determine  $k_m$ ) with faster methods or with slower surfactants. A criterion about whether the adsorption from a given *micellar* solution is fast or slow is provided by the characteristic time of adsorption after a large initial perturbation,  $t_a$ , taken at the CMC:

$$t_a = (\Gamma_{\text{CMC}}/\text{CMC})^2/D_1 \quad [9]$$

Because the adsorption at CMC,  $\Gamma_{\text{CMC}}$ , and the monomer diffusivity,  $D_1$ , have the same order of magnitude for various surfactants, it turns out that  $t_a$  is governed by the value of CMC. In other words, for the same  $\beta$ , the adsorption from the micellar solutions is faster ( $t_a$  is smaller) for surfactants with higher CMC; see Table 1.

**Table 1. Classification of Micellar Surfactant Solutions by Adsorption Time,  $t_a$**

Surfactant	Brij 58	CAPB*	C <sub>12</sub> EO <sub>8</sub>	Triton X-100	SDS + 0.1 M NaCl	DTAB+0.1 M NaBr	AOT
$t_a$ (s)	602	6.2	4.0	0.34	0.0162	0.0012	0.0009

\*CAPB = Cocoamidopropyl betaine

#### 4. Conclusions

Four distinct kinetic regimes of adsorption from micellar solutions exist, called AB, BC, CD, and DE; see Figs. 2 and 4. In regime AB, the fast micellar process governs the adsorption kinetics. In regime BC, the adsorption occurs under diffusion control, because the fast micellar process is equilibrated, while the slow process is negligible. In regime CD, the slow micellar process governs the adsorption kinetics. In regime DE, the adsorption occurs under diffusion control, because both the fast and slow micellar processes are equilibrated. Note that only the regimes BC and DE correspond to purely diffusion processes. For the regimes AB and CD, the rate constants of the fast and slow micellar processes,  $k_m$  and  $k_s$ , respectively, affect the surfactant adsorption kinetics, and could be in principle determined from the fit of experimental data. For the specific experimental examples considered here, the adsorption kinetics corresponds to the diffusion regime BC.

**Acknowledgments.** We gratefully acknowledge the support of Unilever Research & Development, Trumbull, Connecticut, USA, and of the Bulgarian NSF Program “Development of Scientific Infrastructure”. We thank Mr. Vesselin Kolev for his assistance in the manuscript preparation.

## References

1. G.C. Kresheck, E. Hamory, G. Davenport, H.A. Scheraga, *J. Am. Chem. Soc.* 88 (1966) 246-253.
2. E.A.G. Aniansson, S.N. Wall, *J. Phys. Chem.* 78 (1974) 1024-1030.
3. J. Lucassen, *Faraday Discuss. Chem. Soc.* 59 (1975) 76-87.
4. B.A. Noskov, *Kolloidn. Zh.* 52 (1990) 509-514.
5. A. Johner, J.F. Joanny, *Macromolecules* 23 (1990) 5299-5311.
6. C.D. Dushkin, I.B. Ivanov, P.A. Kralchevsky, *Colloids Surf.* 60 (1991) 235-261.
7. P. Joos, J. van Hunsel, *Colloids Surf.* 33 (1988) 99-108.
8. B. Li, P. Joos, M. van Uffelen, *J. Colloid Interface Sci.* 171 (1995) 270-275.
9. P. Joos, *Dynamic Surface Phenomena*, VSP BV, AH Zeist, The Netherlands, 1999.
10. G. Geeraerts, P. Joos, *Colloids Surf. A* 90 (1994) 149-154.
11. K.D. Danov, D.S. Valkovska, P.A. Kralchevsky, *J. Colloid Interface Sci.* 251 (2002) 18-25.
12. K.D. Danov, P.A. Kralchevsky, N.D. Denkov, K.P. Ananthapadmanabhan, A. Lips, *Adv. Colloid Interface Sci.* 119 (2006) 1-16.
13. K.D. Danov, P.A. Kralchevsky, N.D. Denkov, K.P. Ananthapadmanabhan, A. Lips, *Adv. Colloid Interface Sci.* 119 (2006) 17-33.
14. K.D. Danov, P.A. Kralchevsky, K.P. Ananthapadmanabhan, A. Lips, *Colloids Surf. A* **282-283** (2006) 143-161.
15. N.C. Christov, K.D. Danov, P.A. Kralchevsky, K.P. Ananthapadmanabhan, A. Lips, *Langmuir* **22** (2006) 7528-7542.
16. S. Manning-Benson, C.D. Bain, R.C. Darton, *J. Colloid Interface Sci.* 189 (1997) 109-116.